site were calculated. These values, which range from 302 to 317 m/sec, are similar to scores of values determined for acoustic-gravity waves generated by nuclear explosions at different test sites and detected at globally distributed recorders (*1*). They also match the theoretical computations for such propagation (*2*). On the basis of signal appearance and appropriate group velocities (or arrival times), we concluded that signals shown in Fig. 1, a to e, were generated by the eruption of Mount St. Helens.

From pressure amplitudes and periods it is possible to compute the probable explosive energy or yield of the eruption, but not the total energy of the entire event. We used separate theoretical and empirical procedures for this purpose.

1) Posey and Pierce (*3*) developed the following approximate theoretical relationship among energy, pressure perturbation amplitude, and period for an explosion in the atmosphere:

$$E = 13\ P[R \sin (r/R)]^{1/2}\ H_s\ (cT)^{3/2}$$

where E is energy (ergs), P is the first peak-to-trough pressure change (microbars), R is the radius of the earth (centimeters), r is the great circle distance from source to receiver, H_s is the scale height of the atmosphere (taken as 8 km), c is the speed of sound, and T is the wave period (seconds) for the first full wave. From the microbarograph data in Table 1 we computed the yields in megatons (MT) shown in the last column. The average yield is 35 MT.

2) Figure 2a is a plot of pressure amplitude against distance, where the square root of the latter is used because the cylindrical spreading of the gravity waves causes amplitude to decrease as $1/\sqrt{r}$. A straight line has been fitted to the points. Figure 2b is an earlier graph (*4*) of pressure against yield for a number of tests in Novaya Zemlya that were recorded by several instruments in our array of four stations around Palisades, New York. Using the distance from Novaya Zemlya to Palisades (6600 km) in Fig. 2a, we obtain the pressure amplitude for Mount St. Helens for that distance. The resulting value of 190 μbar corresponds to a yield of 35 MT in Fig. 2b, which matches the theoretical calculation above.

3) In another empirical analysis, we used wave period as a tool to estimate yield. In addition to the periods from microbarographs in Table 1, we used values from long-period vertical seismographs at widely distributed locations. Seismic drum records have much higher time resolution than most microbarographs, so that period measurements with good accuracy are obtainable [see, for example, the record from De Bilt in the Netherlands (*5*)]. The data from the seismographs are also given in Table 1. Like the microbarograph signals, the seismograph data yield normal group velocities between source and receivers. Figure 2c shows the period of the first full wave plotted against distance and indicates the dispersion effect described earlier. Only records from stations at least 1000 km from Mount St. Helens were used, to ensure that the lead gravity wave was fully established. Figure 2d shows the period plotted against cube root of yield, where the periods are based on waves from tests at Novaya Zemlya that were recorded on the Palisades array. It is known that wave period varies as the cube root of yield. Only two points in which we have confidence in the yield are plotted, together with zero. Using 6600 km for the distance from Novaya Zemlya, we obtain an equivalent period of 365 seconds from Fig. 2c. This equivalent period corresponds to a yield of 30 MT (from Fig. 2d) for the Mount St. Helens explosion, in good agreement with the theoretical and empirical estimates given above.

On the basis of the best available evidence, we conclude that the explosive yield of the main Mount St. Helens eruption on 18 May 1980 at 1532 GMT was roughly 35 MT (1.48×10^{24} ergs).

Note added in proof: Records from Hawaii and Japan, the only stations with records available to the west of the source, indicate a somewhat lower yield (about 25 MT).

WILLIAM L. DONN
NAMBATH K. BALACHANDRAN
Lamont-Doherty Geological Observatory of Columbia University, Palisades, New York 10964

References and Notes

1. W. Donn and D. Shaw, *Rev. Geophys.* **5**, 53 (1967).
2. N. K. Balachandran, *J. Acoust. Soc. Am.* **48** (Part 2) 211 (1970).
3. J. Posey and A. Pierce, *Nature (London)* **232**, 253 (1971).
4. W. Donn, D. Shaw, A. Hubbard, *IEEE Trans. Nucl. Sci.* **NS-10**, 285 (1963).
5. A. R. Ritsema, *Eos* **61**, 1202 (1980)
6. S. Glasstone and P. Dolan, *The Effects of Nuclear Weapons* (Department of Defense and Department of Energy, Washington, D.C., 1977), p. 43.
7. We are grateful to G. Stilke (University of Hamburg), A. R. Ritsema (Royal Netherlands Meteorological Institute), and W. Hoecker and A. Bedard (National Oceanic and Atmospheric Administration) who provided copies of records from their instruments and to J. Jordan and R. Hunter (USGS Seismology Branch, Denver) for seismograms from the Global Seismic System. This work was supported by grant ATM-08350 from the National Science Foundation, grant NAS 8-33378 from the National Aeronautics and Space Administration, and grant DAAG 0131 from the U.S. Army Research Office. This is Lamont-Doherty Geological Observatory Contribution 3187.

26 January 1981; revised 17 April 1981

Rapid Massive Assembly of Tight Junction Strands

Abstract. *Incubation at 37°C of excised rat prostate tissue results in massive proliferative assembly of new tight junction strands along the entire length of the lateral plasma membranes of the columnar epithelial cells. The new tight junction elements are assembled within 5 minutes and have an average length six times that of those present in the apical tight junction band. Massive assembly occurs in the presence of protein synthesis inhibitors (cycloheximide) or of metabolic uncouplers (dinitrophenol). Thus, proliferative assembly of tight junction strands involves molecular reorganization from a pool of preexisting, probably membrane-associated, components. The fascia occludens and some examples of experimentally induced tight junction proliferation may reflect the massive emergence of tight junction strands when tissue is subjected to diverse stressful conditions.*

The tight junction (occluding junction, zonula occludens) is a specialized intercellular contact between adjacent epithelial cells that assures the physical separation of luminal and intercellular spaces. Current views of tight junction structure derive from the morphological analysis of thin section (*1*) and freeze-fracture (*2*) preparations as seen by electron microscopy. In these studies, the tight junction is described as a network of anastomosing strands visible on the protoplasmic fracture face (*3*), with corresponding furrows observed on the exoplasmic face. As in many other epithelial cells, the strands are predominantly oriented parallel to the edge that separates luminal from lateral regions of the plasma membrane. They generally number less than 15 and may also exist in other regions of the plasma membrane, for example, in places where the polarity of the cells is less marked.

The chemical nature and the supramolecular organization of the tight junction components are virtually unknown, and their biogenesis and assembly are poorly understood. Evidence from freeze-fracture studies indicates that a single or double filament may be the main structural element of this junction (*2*). Studies of its mode of assembly have been hin-

0036-8075/81/0731-0541$00.50/0

dered by the lack of a system in which the formation of the junction might be induced and be amenable to experimental manipulation. We now describe experiments with excised prostate tissue in which we show that massive proliferative assembly of tight junction strands can occur within 3 to 5 minutes, even in the presence of cycloheximide (a protein synthesis inhibitor) or dinitrophenol (a metabolic uncoupler).

For our experiments we used prostate tissues excised from adult male Sprague-Dawley rats that were lightly anesthetized with ether. Each of the experiments was performed at least three times with samples taken from different animals. The tissues were incubated for 0, 3, 5, 15, 30, and 60 minutes in 0.1*M* cacodylate buffer, *p*H 7.4, at 4°C, 37°C, and room temperature. Each specimen was then fixed by immersion in 3 percent glutaraldehyde in 0.1*M* cacodylate buffer, *p*H 7.4, at the temperature of incubation for 3 hours. To rule out the toxic effect of arsenic (from cacodylate), as well as toxicity that might result from incubation and fixation in the absence of Ca^{2+}, Mg^{2+}, K^{+}, and Cl^{-}, we incubated and fixed excised tissues in Tyrode's solution (*4*). Tissues were also incubated and fixed in saline or in 310 mos*M* sodium phosphate buffer, *p*H 7.4. To test the importance of protein synthesis, we incubated the tissues in cycloheximide (100 or 200 μg/ml) in 0.1*M* cacodylate buffer, *p*H 7.4, for 10 minutes at 4°C, then for 5 minutes at 37°C. To test the effect of uncoupling of oxidative phosphorylation, we incubated the tissues in 0.005*M* 2,4-dinitrophenol in 0.1*M* cacodylate buffer, *p*H 7.4, for 10 minutes at 4°C, then for 5 minutes at 37°C. After fixation, the specimens were rinsed in 0.1*M* cacodylate buffer, *p*H 7.4, impregnated in 30 percent glycerol in 0.1*M* cacodylate buffer, *p*H 7.4, placed on gold specimen carriers, frozen in partially solidified Freon 22, freeze-fractured at −110°C, and shadowed at 45° with a platinum-carbon electron gun. The replicas were cleaned, mounted on Formvar-coated grids, and observed at 80 kV with an electron microscope.

The lateral plasma membrane of the prismatic columnar epithelial cell generally has five to seven faces (*5*). When tissues are fixed at 4°C or at room temperature immediately after excision, the membranes are flat, displaying few inter-

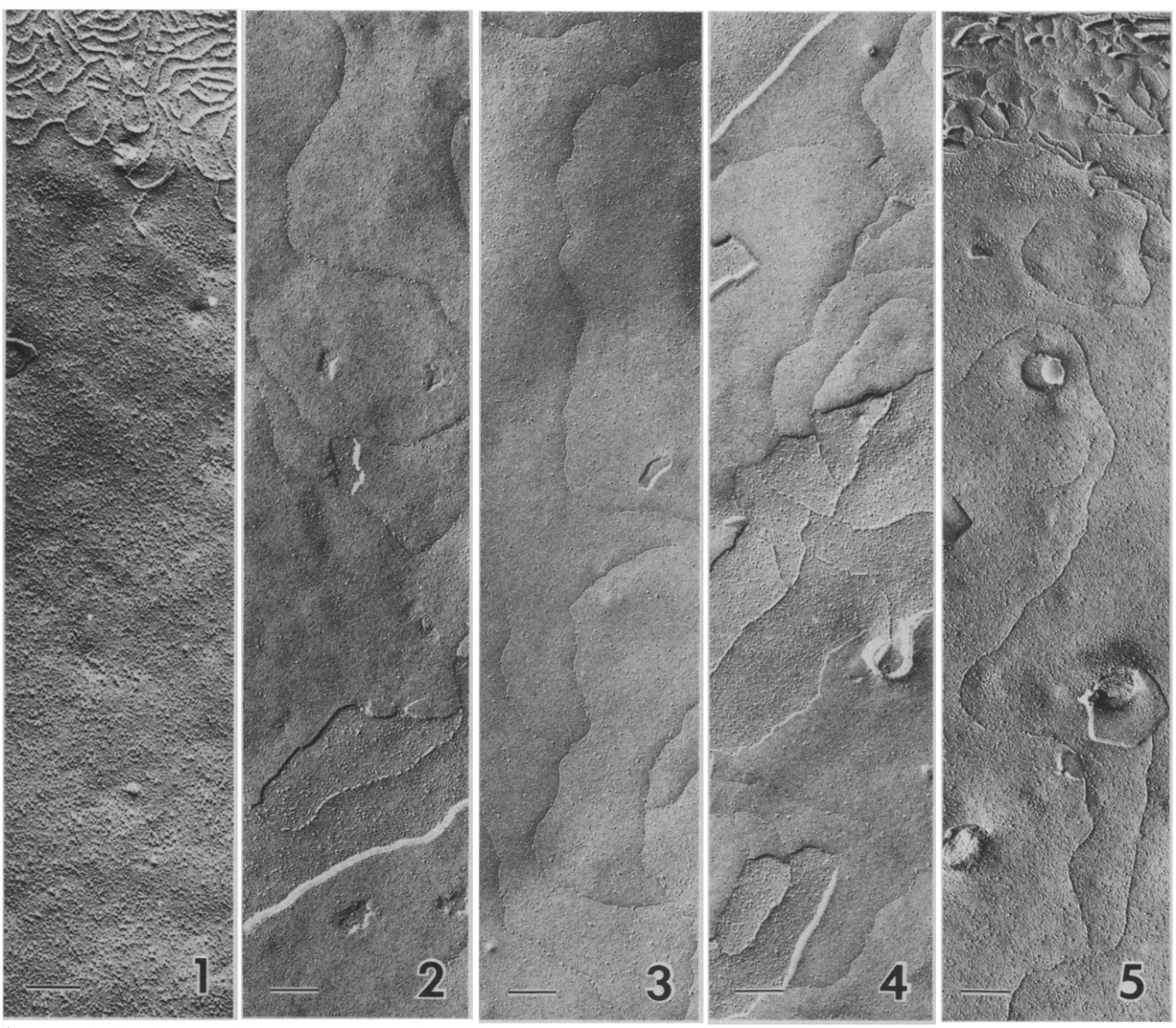

Figs. 1 to 5. Proliferation of tight junction strands on the lateral membranes of rat ventral prostate columnar epithelial cells. Fig. 1. Control. Fig. 2. After incubation for 3 minutes at 37°C. Fig. 3. After incubation for 5 minutes at 37°C. Fig. 4. After incubation in the presence of cycloheximide for 10 minutes at 4°C, then for 5 minutes at 37°C. Fig. 5 After incubation in the presence of dinitrophenol for 10 minutes at 4°C, then for 5 minutes at 37°C. Figs. 1 and 5 show aspects of the top region of the lateral plasma membrane, adjacent to the apical tight junction band; Figs. 2 to 4 show aspects from the mid-region. Scale bar, 0.2 μm.

digitations; and the tight junction, which generally consists of 7 to 15 anastomosed strands, is confined to a narrow (0.5 to 1.0 μm) band contiguous with the apical plasma membrane (Fig. 1). If the excised tissues are fixed at 37°C immediately upon excision, loose strands of the tight junction are observed over approximately one-tenth of the fractured lateral plasma membranes.

After 3 minutes at 37°C (Fig. 2) tight junction strands are frequent in about 50 percent of the fractured lateral membranes, and after 5 minutes at 37°C (Fig. 3) about 90 percent of the fractured lateral membranes show numerous tight junction strands loosely distributed over the entire length of the cell. Identical results were observed in specimens incubated and fixed in cacodylate and phosphate buffers, in Tyrode's solution, or in saline. Massive proliferation was also observed in specimens incubated at 37°C for 10 minutes and fixed with glutaraldehyde in Tyrode's solution that had been equilibrated and continuously bubbled with mixtures of 95 percent O_2 and 5 percent CO_2, 40 percent O_2 and 60 percent CO_2, or 100 percent CO_2. The frequency of new tight junction strands varies within the lateral membrane. In general, the new strands represented independent structures, but some are continuous with those of the apical band (Fig. 5). After 5 minutes and up to 60 minutes of incubation at 37°C, the amount of new tight junction elements is not perceptibly increased. Massive, generalized proliferation is also observed in cells from tissues excised 5 to 10 minutes postmortem. Incubation at 4°C for up to 60 minutes does not result in proliferation of tight junction elements. At room temperature, some loose strands appear after 15 minutes of incubation (not illustrated).

Although the density of the proliferated tight junction strands appears to be low, clearly lower than the density at the apical tight junction band, the strands are spread over the entire area of the fractured lateral membrane. Morphometric analysis (*6*) of micrographs of freeze-fractured lateral plasma membrane after incubation for 5 minutes at 37°C indicates that the average total length of newly formed tight junction strands represents six times (and, in extreme cases, up to 12 times) the length of those present on the apical tight junction band.

Our results cannot be explained without invoking de novo assembly of tight junction strands. Assembly might be achieved either by migration and reorganization of preexisting membrane (and, possibly, cytoplasmic) components or by the incorporation of newly synthesized molecules. The latter alternative appears less likely because of the very short time required (3 to 5 minutes). Experimental confirmation is derived from the observation of intense proliferation of tight junction strands in specimens which, after mincing at 4°C, are incubated in cycloheximide (Fig. 4). Other experiments showed that massive proliferation of tight junction strands occurs in specimens incubated with dinitrophenol (Fig. 5), an indication that the process of assembly does not require the continued operation of oxidative phosphorylation.

Massive assembly of tight junction elements can proceed in the presence of a protein synthesis inhibitor or of a metabolic uncoupler and is observed within a few minutes of the onset of stressful alterations of the cellular environment. In consequence, structural assembly of the tight junction must be carried out from a pool of preexisting components, which probably are, at least in part, elements of the lateral plasma membrane. The contribution of components from presumptive cytoplasmic pools appears to be minor but cannot be assessed. Even in extreme instances of tight junction proliferation, the freeze-fracture morphology of the nondifferentiated regions of the lateral plasma membrane is not altered, and the density of membrane particles appears to be unchanged. Discussion of the possible mechanisms of assembly of tight junction elements is hindered by the absence of plausible structural models for this junction. Migration of membrane components to the loci of junction formation may or may not coexist with alterations of the physical-chemical milieu at those sites; such alterations may be crucial to the process. While massive assembly of tight junctions is taking place, intermediate assembly stages (*7*) are never observed. This suggests that assembly occurs at only a few sites, probably at the tips of the tight junction strands. We believe that membrane lipids have a major role in the structural definition of the tight junction (*8*).

Our experiments cannot identify the underlying biophysical or biochemical alteration of the cellular environment that is responsible for proliferation of tight junction strands. These might include effects within the membrane itself, as well as interactions of tight junction components with cytoplasmic elements; the latter might play a role in the propagation and configuration of the junctional strands. Lowering the intracellular *p*H and, in consequence, disturbing the binding patterns of other ions, in particular Ca^{2+} (*9*), may be involved in many or all of our preparations (in particular those incubated in an atmosphere containing 60 percent or more CO_2). Massive proliferation of tight junction strands is observed even in tissues incubated and fixed with glutaraldehyde in Tyrode's solutions equilibrated with 95 percent O_2 and 5 percent CO_2 or with 100 percent CO_2. It therefore appears unlikely that anoxia or lowering the intercellular *p*H, or both, in themselves constitute necessary conditions for triggering the assembly process. The use of excised epithelial tissues as experimental models should allow kinetic analysis of the de novo assembly of tight junctions.

Multiple tight junction strands along the lateral plasma membranes of epithelial cells were reported as the fascia occludens [that is, they were taken to represent a genuine cellular structure (*10, 11*)] or as instances of experimentally induced proliferation (*12*). These may reflect the massive emergence of tight junction strands that occurs when the tissue is subjected to diverse stressful conditions.

BECHARA KACHAR
PEDRO PINTO DA SILVA*
Laboratory of Pathophysiology,
National Cancer Institute,
National Institutes of Health,
Bethesda, Maryland 20205

References and Notes

1. M. G. Farquhar and G. E. Palade, *J. Cell Biol.* **17**, 375 (1963); *ibid.* **26**, 263 (1965); D. A. Goodenough and J. P. Revel, *ibid.* **45**, 272 (1970); D. S. Friend and N. B. Gilula, *ibid.* **53**, 148 (1972); N. B. Gilula, *Dev. Biol.* **50**, 142 (1976).
2. J. P. Chalcroft and S. Bullivant, *J. Cell Biol.* **47**, 49 (1970); D. S. Friend and N. B. Gilula, *ibid.* **53**, 758 (1972); L. A. Staehelin, *J. Cell Sci.* **13**, 763 (1973); M. Simionescu, N. Simionescu, G. Palade, *J. Cell Biol.* **67**, 863 (1975); *ibid.* **68**, 705 (1976); M. Simionescu and N. Simionescu., *ibid.* **74**, 98 (1977).
3. D. Branton *et al., Science* **190**, 54 (1975).
4. C. Peracchia, *J. Cell Biol.* **72**, 628 (1977).
5. L. J. A. Didio, *Anat. Anz.* **128**, 170 (1971); G. Aumuler, in *Handbuch der Mikroskopischen. Anatomie des Menschen* (Springer-Verlag, Berlin, 1979), vol. 7, p. 6.
6. The measured average length of apical strand per micrometer of apical tight junction band was 11 μm. The average length of proliferated lateral junction strand per micrometer of longitudinal band along the entire lateral length of prismatic cell was 68 μm; this value was estimated by measuring the length of tight junction strands on 15 different 5-μm^2 areas of fractured lateral membrane and extrapolating to the average area of lateral membrane per micrometer of cell perimeter [1 μm × 35 μm (average length of prismatic cell) = 35 μm^2]. The proliferation index (68/11) is 6.2.
7. J. B. Wade and M. J. Karnovsky, *J. Cell Biol.* **60**, 168 (1974); R. Montesano, D. S. Friend, A. Perrelet, L. Orci, *ibid.* **67**, 310 (1975); H. Fujisawa, H. Morioka, H. Nakamura, K. Watanabe, *J. Cell Sci.* **22**, 597 (1976); R. Dermietzel *et al., Cell Tissue Res.* **181**, 427 (1977); L. W. Tice, R. L. Carter, M. C. Cahill, *Tissue Cell* **9**, 395 (1977); R. Meyer, C. Posalaky, D. McGinley, *J. Ultrastruct. Res.* **61**, 271 (1977); M. Porvaznik, R. G. Johnson, K. D. Sheridan, *J. Supramol. Struct.* **10**, 13 (1979).
8. P. Pinto da Silva and B. Kachar, in preparation.
9. B. Rose and R. Rick, *J. Membr. Biol.* **44**, 377 (1978); C. Peracchia, *Nature (London)* **271**, 669

(1978); ——— and L. L. Peracchia, *J. Cell Biol.* **87**, 719 (1980).
10. L. A. Staehelin, *J. Cell Sci.* **13**, 763 (1973); *Int. Rev. Cyt.* **39**, 191 (1974); F. Suzuki and T. Nagano, *Anat. Rec.* **191**, 503 (1978).
11. S. Knutton, A. R. Limbrick, J. D. Robertson, *Cell Tissue Res.* **191**, 449 (1978).
12. Tight junction proliferation was induced by (i) incubation in glycerol solutions (*11*) or in Ca^{2+}-free media [P. Galli, A. Brenna, P. De Camilli, J. Meldolesi, *Exp. Cell. Res.* **99**, 178 (1976)]; (ii) prolonged administration of *N*-nitrosomorpholine [H. Robeneck, M. Döldissen, H. Themann, *J. Ultrastruct. Res.* **70**, 82 (1980)] or phalloidin [R. Montesano, G. Gabbiani, A. Perrelet, L. Orci, *J. Cell Biol.* **68**, 793 (1976)]; (iii) sublethal gamma irradiation [M. Porvaznik, *Radiat. Res.* **78**, 233 (1979)]; (iv) exposure of the tissue to organ culture conditions [J. L. Carson *et al.*, *J. Ultrastruct. Res.* **70**, 70 (1980)]; (v) rapidly proliferating cells in regenerating tissue [A. G. Yee, *J. Cell Biol.* **55**, 294a (1972)]; and (vi) retinoic acid–induced metaplasia [P. M. Elias and D. S. Friend, *ibid.* **68**, 173 (1976)].
* Send reprint requests to Laboratory of Pathophysiology, Building 10, Room 5850, National Cancer Institute, National Institutes of Health, Bethesda, Md. 20205.

10 March 1981

Diketopiperazine Formation During Investigations of Amino Acid Racemization in Dipeptides

Abstract. *The formation of diketopiperazines from the dipeptides isoleucylglycine and glycylisoleucine was investigated at 132°C over the* p*H range ~ 2 to 10. At* p*H 6.2, ~ 50 percent of the original dipeptides were converted to the diketopiperazines during the heating experiments. Hydrolysis of the diketopiperazines can yield either the original dipetide or an inverted dipeptide product. The isoleucine in the diketopiperazines was the most highly epimerized component in the system. Previous racemization and epimerization studies with dipeptides have not taken into account the formation of diketopiperazines and, as a result, the conclusions about the mechanism and geochemical implications of amino acid racemization in dipeptides will require revision.*

Investigations of the kinetics of racemization of dipeptides have been suggested to provide new insights into the mechanism of amino acid racemization in peptides and in calcareous fossils. On the basis of the studies of epimerization of isoleucine in several di- and tripeptides at ~ *p*H 6 and 152°C Kriausakul and Mitterer (*1*) reported that NH_2-terminal isoleucine epimerizes faster than COOH-terminal isoleucine. Smith and de Sol (*2*) studied the racemization of 37 dipeptides at *p*H 7.6 and 122°C. Their results indicate that in general COOH-terminal amino acids racemize faster than NH_2-terminal amino acids. De Sol and Smith explained these results by invoking inductive effects, by neighboring group stabilization of the carbanion intermediate, and by steric effects on the solvation of the carbanion.

We felt that the mechanistic conclusions or geochemical implications of these dipeptide results were premature because of the necessity of first investigating *p*H effects on amino acid racemization rates in various dipeptides. These studies are important in order to deduce which ionic species of the dipeptide is undergoing racemization at a particular *p*H and temperature. For example, elevated temperature experiments (*3*) with free amino acids buffered at various *p*H values indicate that at *p*H 7.6 there is a mixture of ionic species racemizing and that these various ionic species have greatly differing racemization rates. In order to demonstrate which factors control the relative racemization rates of free amino acids, it was necessary to determine and compare the rates for a particular ionic species; comparisons using the observed racemization rates at a particular *p*H give misleading conclusions (*3*).

Besides the dipeptide ionic species problem, there is also the complication that dipeptides may cyclize to form diketopiperazines. Hydrolysis of the diketopiperazine may either regenerate the original dipeptide or create an inverted dipeptide. It is well known that dipeptide esters and amides easily cyclize to diketopiperazines. At 25°C the rate of cyclization competes favorably with ester or amide hydrolysis (*4*). Brewerton *et al.* (*5*) observed extensive sequence inversion in some dipeptides in 2*M* HCl at 84° to 114°C. Long *et al.* (*6*) observed that divalent metal ions catalyzed cyclization of glycylglycine at *p*H 3.8 to 6.0 at 91° to 114°C. These investigations demonstrate the quantitative importance of diketopiperazine formation and dipeptide sequence inversion relative to peptide bond hydrolysis. Furthermore, amino acid residues in diketopiperazines are rapidly racemized at room temperature in dilute alkali (*7*).

In order to investigate the effects that *p*H has on the racemization of dipeptides and the possible formation of diketopiperazines we have conducted heating experiments with glycylisoleucine and isoleucylglycine in various buffered solutions ranging from *p*H ~ 2 to 10 (ionic

Table 1. Diketopiperazine formation, dipeptide inversion, and epimerization in glycylisoleucine and isoleucylglycine at 131°C in the *p*H range ~ 2 to 10. Under the experimental conditions, the extent of hydrolysis of the dipeptides to free amino acids was less than 5 percent in all cases. Abbreviations: allo/iso, alloisoleucine/isoleucine; diketo, 3-isobutyl-2,5-piperazinedione.

*p*H at 131°C*	Heating time (hours)	Original dipeptide allo/iso	Inversion (%)†	Inverted dipeptide allo/iso	Diketo (%)†	Diketo allo/iso	Total allo/iso‡
			Glycylisoleucine				
2.11	72	0.10	71	0			
3.42	72	0.12	62	0	80	< 0.05	~ 0.08
4.85	72	0.15	63	0	77	~ 0.08	~ 0.05
5.55	72	0.16	49	0.06	48	0.21	0.14(0.15)
6.36	24	0.09	49	0.26			
6.36	48	0.19	76	0.59	58	0.79	0.59(0.66)
7.79	24	0.04	60	1.3			
7.79	48	0.07	74	1.4	11	1.23	0.81(0.81)
8.66	24	0.02	13	1.4			
8.66	48	0.03	30	1.4	0.01	1.4	0.30(0.25)
9.56	24	0.02	7	1.4			
			Isoleucylglycine				
2.11	12	0.01	48	0.03			
3.42	12	0.02	34	0.32	28	~ 0	< 0.05
4.85	12	0.02	4	0.64			
5.55	8	0.02	14	1.0	36	< 0.05	< 0.05
6.36	12	0.15	17	0.22	61	0.28	0.28(0.23)
7.79	8	0.36	4	0.15			
7.79	12	0.58	6	0.14	18	1.0	0.73(0.69)
8.66	12	0.16	3	0.20	12	1.4	0.29(0.24)
9.56	8	0.11	3	§			

*The *p*H values of the buffers at 131°C were extrapolated with the use of the equations given by Bates (*12*). †Percent inversion is tabulated relative to the total amount of dipeptide recovered from the heated samples [inverted/(original + inverted)] excluding the diketopiperazine fraction. The percent diketo is tabulated relative to the total amount of dipeptide and diketopiperazine recovered from the heated sample [diketo/(diketo + original + inverted)]. ‡The allo/iso values given in parentheses were calculated from the allo/iso ratios determined for the dipeptide and diketopiperazine fractions and the relative abundances of each component analyzed. §No inverted product was detected.

0036-8075/81/0731-0544$00.50/0